BIOCHEMISTRY
including biophysical chemistry & molecular biology

Article

pubs.acs.org/biochemistry

pK_a Shifting in Double-Stranded RNA Is Highly Dependent upon Nearest Neighbors and Bulge Positioning

Jennifer L. Wilcox[†,‡] and Philip C. Bevilacqua*[,‡]

[‡]Department of Chemistry and Center for RNA Molecular Biology, Pennsylvania State University, University Park, Pennsylvania 16802, United States

Supporting Information

ABSTRACT: Shifting of pK_a's in RNA is important for many biological processes; however, the driving forces responsible for shifting are not well understood. Herein, we determine how structural environments surrounding protonated bases affect pK_a shifting in double-stranded RNA (dsRNA). Using ^{31}P NMR, we determined the pK_a of the adenine in an A$^+$·C base pair in various sequence and structural environments. We found a significant dependence of pK_a on the base pairing strength of nearest neighbors and the location of a nearby bulge. Increasing nearest neighbor base pairing strength shifted the pK_a of the adenine in an A$^+$·C base pair higher by an additional 1.6 pK_a units, from 6.5 to 8.1, which is well above neutrality. The addition of a bulge two base pairs away from a protonated A$^+$·C base pair shifted the pK_a by only ~0.5 units less than a perfectly base paired hairpin; however, positioning the bulge just one base pair away from the A$^+$·C base pair prohibited formation of the protonated base pair as well as several flanking base pairs. Comparison of data collected at 25 °C and 100 mM KCl to biological temperature and Mg^{2+} concentration revealed only slight pK_a changes, suggesting that similar sequence contexts in biological systems have the potential to be protonated at biological pH. We present a general model to aid in the determination of the roles protonated bases may play in various dsRNA-mediated processes including ADAR editing, miRNA processing, programmed ribosomal frameshifting, and general acid−base catalysis in ribozymes.

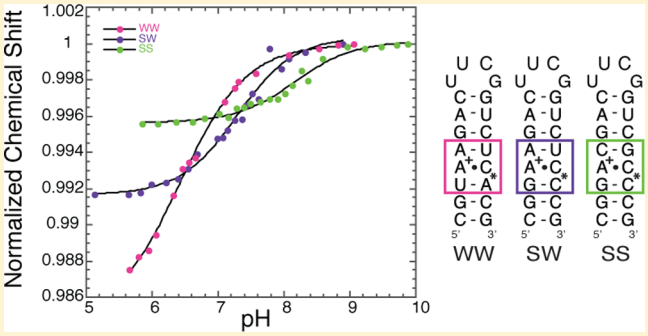

Single-stranded DNA and RNA nucleobases are typically uncharged, with pK_a values of 3.5 and 4.2 for A and C, respectively, and 9.2 for G and T/U.[1] Watson−Crick base pairing shifts the pK_a values even further away from physiological pH because the protons are engaged in hydrogen bonding.[2,3] In some noncanonical base pairs, however, pK_a values are shifted toward neutrality,[4] thereby allowing these nucleobases to play important roles in biological processes, such as general acid−base catalysis[4] and programmed ribosomal frameshifting.[5] For example, in the HDV ribozyme, the pK_a of C75 is shifted to neutrality,[6−8] whereas a pseudoknot element in beet western yellows virus has a pK_a greater than neutrality,[9,10] and a number of double-stranded DNA (dsDNA) elements have pK_a values near neutrality.[10,11] In addition, miRNA and adenosine deaminase (ADAR) processing act on double-stranded RNA (dsRNA) substrates[12−16] that contain motifs that likely ionize and regulate function, such as A$^+$·C wobbles. Although significant research has been done to determine how protonated bases participate in these processes, many protonated bases likely remain unidentified.

Numerous studies reveal that RNA and DNA stability depends on the identity of nearest neighbors.[17,18] In addition, pK_a shifting has been linked to changes in RNA folding.[19] However, the influence of nearest neighbors on pK_a shifting in dsRNA has received only limited attention. In this study, we investigate the effect that the structural environment surrounding a protonated base pair has on pK_a shifting in RNA. Using ^{31}P NMR with a phosphorothioate-labeled RNA sample,[20] we analyze how changing the strength of nearest neighbor base pairing and the addition of a bulge at various positions affects the pK_a of an A$^+$·C wobble.

MATERIALS AND METHODS

Preparation of RNA Samples. RNA oligonucleotides were synthesized by the manufacturer (Dharmacon, Lafayette, Colorado) and deblocked according to the manufacturer's protocol. Oligonucleotides were dialyzed as previously described.[11] Purity of RNA samples was confirmed by denaturing PAGE with SYBR Gold staining after completion of an entire pH titration. Samples migrated as expected relative to one another and to a size marker. RNA sequences were as provided below.

After dialysis, RNA was brought up in a 500 μL volume that contained between 0.88 and 1.26 mM RNA in 100 mM KCl and 10% D_2O. Titrations were conducted in the absence of buffer so as to allow for small pH changes upon addition of acid or base. Slight buffering of the system was provided by the high

Received: June 15, 2013
Revised: September 15, 2013
Published: October 7, 2013

```
WW:              5′ CGU AAG ACU UCG GUC UCA CG
WW′:             5′ CGU AUG ACU UCG GUC ACA CG
SW:              5′ CGG AAG ACU UCG GUC UCC CG
SW′:             5′ CGG AUG ACU UCG GUC ACC CG
SS:              5′ CGG ACG ACU UCG GUC GCC CG
Bulge-0(=SS′):   5′ CGG AGG ACU UCG GUC CCC CG
Bulge-1:         5′ CGG AGA CGC UUC GGC GCC CCG
Bulge-2:         5′ CGG AGC AGC UUC GGC GCC CCG
```

concentrations of RNA itself. The sample was renatured by heating at 90 °C for 2 min and then cooled on the benchtop for 15 min. The pH was measured using a Hach IQ 160 meter with an NMR tube microprobe. The probe was calibrated before pH determination with pH 7 and 10 standards (BDH General-VWR), which were replaced periodically. After renaturation of the RNA, the pH was adjusted to the desired alkalinity with small volumes of KOH to begin the titration in the range of pH 9−10. Higher pH values were avoided so as to not alkaline denature or hydrolyze the RNA.

^{31}P NMR Titration of RNA. NMR spectra were collected on a Bruker AV-3-600 MHz NMR spectrophotometer using previously described parameters[11] and analyzed using TopSpin software. An internal coaxial tube containing 1% trimethyl phosphate (TMP) in 5% D_2O was used as a reference and set to 0 ppm for each spectrum. For each pH data point, the pH was determined in the NMR tube; the internal coaxial tube was reinserted; and an NMR spectrum was collected at 25 °C (unless otherwise noted). After each spectrum was acquired, the coaxial tube was removed and the pH was redetermined. The pH value used in analysis was the average of the two recorded values. Small volumes of concentrated HCl were used to increase the acidity of the solution throughout the titration. While NMR spectra were being collected, the pH probe remained submerged in pH 7 standard. If the observed pH varied by more than 0.05 pH units from the standard value, the probe was recalibrated. Once the pH values being reported reached approximately 7, the probe was recalibrated with the pH 4 and 7 standards (BDH General-VWR). For each pH value, the chemical shifts of the two phosphorothioate resonances were monitored as a function of pH and fit to the Henderson−Hasselbalch equation (1) using KaleidaGraph software, and the pK_a and Hill coefficient were determined and are provided in Table 1.

$$S = S_A + \frac{S_{HA} - S_A}{1 + 10^{n(pH - pK_a)}} \quad (1)$$

^{1}H NMR of RNA. To identify base pairing in various RNA constructs, one-dimensional (1D) imino proton (^{1}H) spectra were collected on a Bruker AV-3-600 MHz NMR spectrophotometer with a CTI cryoprobe. The temperature was held at 276 K to reduce proton exchange and promote sharpness of peaks. Water suppression pulse programs were employed, as described previously.[11] Samples for ^{1}H NMR were ∼0.25−0.5 mM RNA, 100 mM KCl, and 10% D_2O. Data were analyzed with TopSpin software.

UV Melts of RNA. RNA (∼1.5 μM) was melted in the background of 100 mM KCl and 10 mM buffer (Bis−Tris−propane pH 5.03 and 8.79 or 9.22, or MES pH 6.13; pH was determined at room temperature) in 1 cm path length quartz cuvettes.

Table 1. pK_a Values of RNA Oligonucleotides with Varying Nearest Neighbors or Proximity of Bulges to the A$^+$·C Wobble

construct	pK_a[a]	Hill coefficient[a]
WW	6.51 ± 0.04[b]	1.01 ± 0.07[b]
WW′	7.09 ± 0.03[b]	0.91 ± 0.06[b]
SW	7.28 ± 0.08[b]	0.86 ± 0.27[b]
SW′	7.84 ± 0.05[b]	1.00 ± 0.12[b]
SS	8.10 ± 0.06[b]	1.09 ± 0.16[b]
SS′ (=Bulge-0)	8.00 ± 0.06	1.34 ± 0.23
Bulge-0 (=SS′)	8.00 ± 0.06	1.34 ± 0.23
Bulge-2	7.46 ± 0.17	1[c]
Bulge-1	no pK_a[d]	no Hill coefficient[d]

[a]Curves were fit to the Henderson−Hasselbalch equation (eq 1) to determine pK_a values and Hill coefficients. [b]pK_a values and Hill coefficients listed are the averages from the two diastereomer peaks. If a value is not superscripted, only one peak showed sufficient change in signal to yield a pK_a. Error is from the fits and propagated conservatively as the average of the errors of each measurement. The number of reliable significant figures in pK_a values is two, but an extra figure is provided to avoid round-off errors in calculations. [c]For fitting Bulge-2, the Hill coefficient was set to 1 in the Henderson−Hasselbalch equation. [d]No pK_a was reported due to either a linear or noisy response to pH. All values in this table were measured at 100 mM KCl and 25 °C. Titrations are provided in Figures 2, S1, S4, and S5 of the Supporting Information.

Buffer pH values were chosen such that the pH was at least 1 unit removed from the pK_a of the construct as measured above, so as to favor the protonated or deprotonated states as desired. Samples were renatured by heating to 90 °C for 2 min and then cooling to room temperature for 15 min. UV monitored thermal denaturation experiments (melts) were conducted at 260 nm on a Gilford Response II spectrophotometer equipped with a temperature controlled microcuvette assembly. Absorbances were collected from 5 to 95 °C in 0.5 °C increments. Data were analyzed using KaleidaGraph software as previously described.[21] Five-point smoothing was done prior to taking first derivatives. Values for $\Delta G°$ were calculated at 37, 50, and 70 °C to facilitate comparisons amongst different constructs at various temperatures. All thermodynamic parameters are provided in Table S1 of the Supporting Information, and select values at 50 °C are provided in Table 2 because this temperature is close to, but below, the T_m. Errors in free energy are typically 0.1 kcal/mol.[21] The melting temperature (T_m) was independent of RNA concentration at both low and high pH (see Table S2 of the Supporting Information), supporting that the RNA was melting as a monomer.

RESULTS AND DISCUSSION

Nearest Neighbor Base Pairing Strength Has a Strong Effect on pK_a Shifting. To investigate the effect of nearest neighbor base pairing strength on pK_a shifting, we determined the pK_a of adenine in an A$^+$·C wobble with two weak (A−U) W−C base pairs ("WW"), one strong (G−C) and one weak (A−U) W−C base pair ("SW"), or two strong (G−C) W−C base pairs ("SS") as the nearest neighbors (Figure 1). Initial experiments are in 100 mM KCl and at 25 °C. Representative NMR titrations are shown in Figure 2, full titrations are provided in Figure S1 of the Supporting Information, and pK_a and Hill coefficient values are given in Table 1. An A$^+$·C wobble with two weak (A−U) base pairs as nearest neighbors (in WW) had a pK_a of 6.51. This value is shifted ∼3 units upward from free adenine but was still the least shifted in this series. The combination of a strong (G−C) and a weak (A−U) base pair (in SW) resulted in an intermediate pK_a

dx.doi.org/10.1021/bi400768q | Biochemistry 2013, 52, 7470−7476

Table 2. Thermodynamic Parameters from UV Monitored Thermal Denaturation

construct	pH[a]	T_m (°C)[b]	ΔG°_{50} (kcal/mol)[b]
WW	5.03	66.4 ± 0.17	−2.40
	8.79	68.2 ± 0.32	−1.52
SW	6.13	77.7 ± 0.08	−4.97
	8.79	72.6 ± 0.07	−3.58
SS	6.13	89.7 ± 1.73	−5.81
	9.22	77.0 ± 0.04	−4.69
SS′	6.13	87.2 ± 0.57	−6.27
	9.22	80.3 ± 0.08	−5.81

[a]Melts were conducted at the specified pH, which was determined at room temperature. [b]T_m and ΔG°_{50} values were determined from fits of absorbance curves. Error in T_m is from the fits. Typical error in ΔG° values are ∼0.1 kcal/mol. Full thermodynamic parameters are provided in Table S1 of the Supporting Information.

of 7.28, suggesting a dependence of pK_a on nearest neighbor base-pairing strength. Continuing this trend, flanking the A$^+$·C base pair with two strong (G−C) base pairs (in SS) gave the largest pK_a of 8.10. Notably, changing the nearest neighbors from two A−U base pairs to two G−C base pairs caused an upward pK_a shift of 1.6 units. We conclude that additional structural stability contributed by neighboring base pairs may enable a more shifted pK_a.

Overlay of the titration curves of the WW, SW, and SS RNA constructs reveals distinct differences in the range of the chemical shift (Figure 2). For the upfield-shited diastereomer peak, the WW curve shows an increase in normalized chemical shift upon deprotonation of 0.807 ppm, the greatest of the three constructs, whereas the SS curve shows a chemical shift increase of just 0.234 ppm. Likewise the SW construct with the intermediate pK_a, has an intermediate range of 0.453. (Similar trends are found for the downfield-shifted diastereomer (Figure S1 of the Supporting Information)). We infer that the lesser chemical shift ranges of the SW and especially SS constructs are due to the structural rigidity conferred by the stronger G−C base pairs. This rigidity may limit the change in the chemical environment of the phosphorothioate reporter. Likewise, the two weak A−U nearest neighbors in the WW construct may promote flexibility and thus a larger difference in chemical environment between the protonated and deprotonated states, thus leading to a larger chemical shift range.

To understand the thermodynamic driving forces for the nearest neighbor dependence observed in pK_a shifting, UV-monitored thermal denaturation experiments were performed on the WW, SW, and SS constructs. Thermodynamic parameters are provided in Tables 2 and S1 of the Supporting Information and melts are given in Figures S2 and S3 of the Supporting Information. In all constructs, a more favorable ΔG°_{50} is observed at the lower pH, consistent with protonation and base pair formation of the A$^+$·C wobble. In addition, at both low and high pH, there is an increase in stability upon going from WW to SW to SS constructs, as found for pK_a shifting. Thus, addition of G−C base pairing contributes both to the stability of the construct and shifting of the pK_a.

So far, we have described pK_a and stability effects due to large differences in base pairing strength, going from weak to strong base pairs. We also wished to examine the dependence of these parameters on sequences within the same types of base pairs. Parameters of WW, SW, and SS were thus compared to WW′, SW′, and SS′ constructs in which the base pair below the A$^+$·C wobble remained constant and the base pair above the A$^+$·C

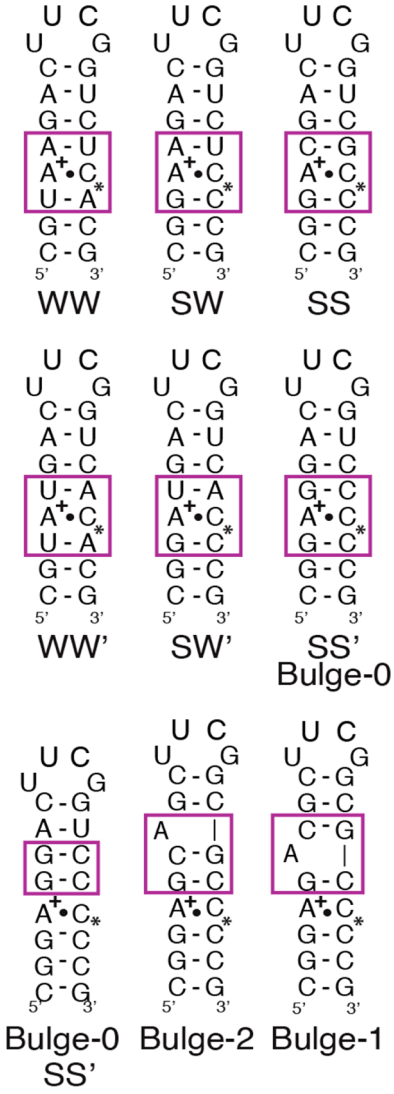

Figure 1. Protonated RNA oligonucleotides used in ^{31}P-detected pH titrations. To test the dependence of the pK_a on nearest neighbors, constructs WW and WW′ with two weak A−U base pairs neighboring the A$^+$·C wobble were compared, SW and SW′ with one strong G−C and one weak A−U base pair neighboring the A$^+$·C wobble were compared, and SS and SS′ with two strong G−C base pairs neighboring the A$^+$·C wobble were compared. To assess effects of a structural defect on the pK_a, constructs with a bulge two (Bulge-2) or one (Bulge-1) base pair(s) away from the A$^+$·C wobble, along with an analogous RNA with no bulge (Bulge-0, also referred to as "SS′"), were compared. The asterisks denote the position of the phosphorothioate substitution used for detection by ^{31}P NMR.

wobble was reversed in order (Figures 1, S4, and S5 of the Supporting Information). The pK_a values for this set of six sequences are provided in Table 1. For all constructs, there was a distinct clustering of pK_a values, with WW and WW′ having the least shifted pK_a values of 6.51 and 7.09, respectively, SW and SW′ having intermediate shifted pK_a values of 7.28 and 7.84, respectively, and SS and SS′ possessing the most shifted pK_a values of 8.10 and 8.00, respectively. This clustering of pK_a values with base pairing strength fully supports the conclusion that nearest neighbor base pairing strength affects pK_a shifting. We also measured thermodynamic parameters for SS′, and its ΔG°_{50} and T_M values were similar to those for SS (Table 2), consistent with similar pK_a values (Table 1).

dx.doi.org/10.1021/bi400768q | Biochemistry 2013, 52, 7470−7476

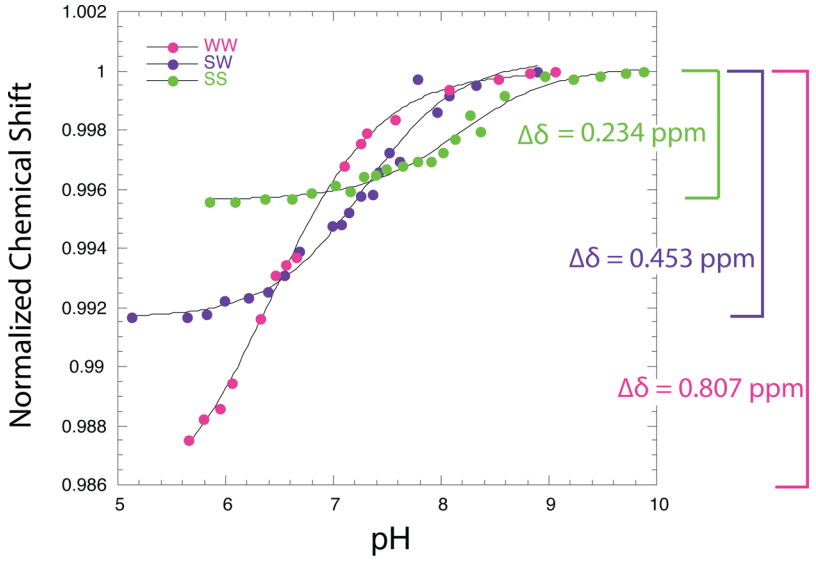

Figure 2. Overlay of ^{31}P NMR-detected pH titrations of WW (pink), SW (purple), and SS (green) RNA constructs. The upfield-shifted diastereomer peak is shown, whereas both diastereomer peaks are provided in Figure S1 of the Supporting Information. Titration curves were fit to the Henderson–Hasselbalch equation, and the pK_a and Hill coefficient are provided in Table 1. Actual changes in chemical shift between the protonated and deprotonated states for the upfield-shifted diastereomer peak are given in the figure; similar trends were found for the downfield-shifted peak (see Figure S1 of the Supporting Information). All values are at 100 mM KCl and 25 °C.

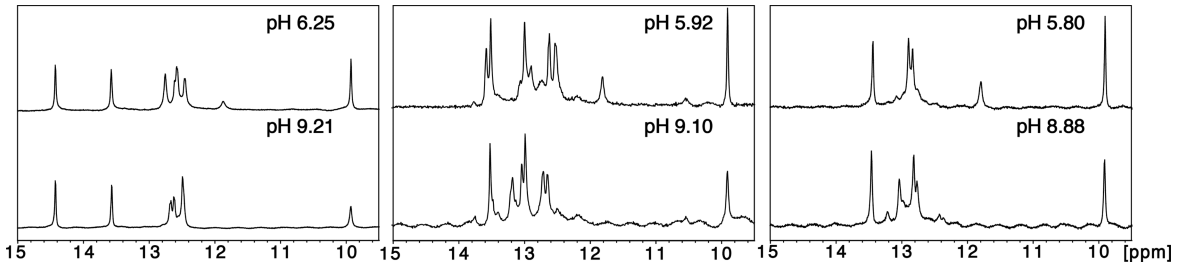

Figure 3. Exchangeable ^{1}H NMR of Bulge-0 (left), Bulge-2 (middle), and Bulge-1 (right) from 9.6 to 15 ppm. Spectra were collected at 3 °C to limit exchange of imino protons at the indicated low pH (top row) and high pH (bottom row). All spectra are in the background of 100 mM KCl.

pK_a Shifting Is Dependent upon Bulge Proximity. In addition to different nearest neighbors, many biological dsRNAs have bulges proximal to A$^+$·C wobbles. To examine the effect of disruption of helical structure near a protonated base, we determined the pK_a in three constructs: "Bulge-1" with an A-bulge one base pair away from an A$^+$·C wobble, "Bulge-2" with an A-bulge two base pairs away from an A$^+$·C wobble, and "Bulge-0", an analogous RNA construct with no bulge near the A$^+$·C wobble. The pK_a values for this set of sequences are provided in Table 1. Bulge-0 (=SS′) has a highly shifted pK_a of 8.00, as described above, and Bulge-2 has a fairly similar pK_a of 7.46 (Figure S5 of the Supporting Information). Thus, positioning the bulge two base pairs away from the A$^+$·C has a relatively minor effect on the pK_a, lowering it just ∼0.5 units from the perfectly double-stranded construct, with a value still above neutrality. Strikingly, no pK_a was observed for Bulge-1. This effect was further investigated using ^{1}H NMR.

Base pairing in Bulge-0, Bulge-1, and Bulge-2 constructs was analyzed by ^{1}H NMR at both low (∼6) and high (∼9) pH (Figure 3). G–C and A–U imino protons resonate at ∼12–13 and ∼13–15 ppm, respectively.[22] Of the three constructs analyzed, only Bulge-0 (Figure 3) has a resonance near 14.4 ppm in spectra at both low and high pH, consistent with its unique A–U base pair. An intense resonance near 10 ppm in all three bulge constructs at both low and high pH is due to an imino proton from position 4 of the cUUCGg loop (closing base pair in lower case) and a weaker resonance near 11.8 ppm at low pH (where there is less chemical exchange) is from an imino proton at position 1 of the cUUCGg loop.[23,24] These resonances, which are diagnostic of a hairpin UUCG tetraloop but not a duplex UUCG internal loop, confirm the formation of a hairpin rather than a duplex.[23−25] This observation is in line with lack of dependence of the T_m from UV melts on RNA concentration (Table S2 of the Supporting Information) and shows that the monomeric state of the RNA extends to NMR concentrations.

Inspection of the imino proton spectra also reveals an increase in chemical shift dispersion upon lowering pH for the Bulge-0 and Bulge-2 samples (Figure 3). This behavior is indicative of base pairing adjacent to and at the base paired A$^+$·C wobbles, as described previously for DNA hairpins with an A$^+$·C wobble in the stem.[22] Bulge-1, on the other hand, has distinctly fewer resonances in the imino region of the spectrum, both at low and high pH, correlating to fewer base pairs and lack of an observed pK_a in the ^{31}P NMR-detected pH titration. Apparently, positioning the bulge one base pair away from the A$^+$·C wobble is disruptive to the stem, likely prohibiting formation of the G–C base pairs below and above the A$^+$·C wobble. Indeed, the imino resonances for the Bulge-1 construct at low pH are consistent

dx.doi.org/10.1021/bi400768q | *Biochemistry* 2013, 52, 7470−7476

with the two most upfield resonances coming from the UUCG tetraloop (see above), while the three more downfield resonances likely arise from those G−C base pairs that are most protected from solvent: the two nearest the UUCG tetraloop and possibly the central G−C in the lower stem. As stated above, these data support partial or complete loss of multiple base pairs in the Bulge-1 construct.

Table 3. Comparison of pK_a Values of RNA Oligonucleotides at Various Temperatures

construct	T (°C)	pK_a[a]	Hill coefficient[a]
WW′	25	7.09 ± 0.03	0.91 ± 0.06
	37	7.04 ± 0.03	1.01 ± 0.05
SW′	25	7.84 ± 0.05	1.00 ± 0.12
	37	7.69 ± 0.04	0.96 ± 0.05
SS	25	8.10 ± 0.06	1.09 ± 0.16
	37	8.14 ± 0.07	0.93 ± 0.12

[a]Curves were fit to the Henderson−Hasselbalch equation (eq 1) to determine pK_a values and Hill coefficients. The pK_a values and Hill coefficients listed are the averages from the two diastereomer peaks. Error is from the fits and propagated conservatively as the average of the errors of each measurement. Values are at 100 mM KCl and either 25 or 37 °C as indicated. Titrations are provided in Figures 2, S1, S4, S6, and S7 of the Supporting Information.

pK_a Shifting Is Maintained at Biological Temperature and Mg^{2+} Concentration. In an effort to test if the pK_a values change under biological conditions, we compared the pK_a results above measured under our standard experimental conditions of 100 mM KCl and 25 °C to more biological conditions of 100 mM KCl and 37 °C or 0.5 mM Mg^{2+}/100 mM K^+. The dependence of pK_a value on temperature is provided in Table 3. Titrations under these conditions showed no significant dependence of the pK_a on the temperature or magnesium concentration (Figures 4, S6, and S7 of the Supporting Information). For example, increasing the temperature from 25 to 37 °C shifted the pK_a from 7.09 to 7.04 in the WW′ construct, from 7.84 to 7.69 in the SW′ construct, and from 8.10 to 8.14 in the SS construct. The SW′ construct displayed the largest, yet still fairly minimal, temperature dependence, in which increasing the temperature to 37 °C from our standard experimental temperature of 25 °C decreased the pK_a by only 0.15 units. The very similar pK_a values observed at 25 and 37 °C for all three constructs supports the conclusion that, even though their melting temperatures vary, all hairpins are fully formed at both 25 and 37 °C, as expected given that the T_m values for weak−weak to strong−strong constructs are all above 65 °C (Table 2).

Adding magnesium to 0.5 mM Mg^{2+}, which is near the intracellular biological concentration of Mg^{2+} in mammals,[26−29] while maintaining the standard experimental temperature of

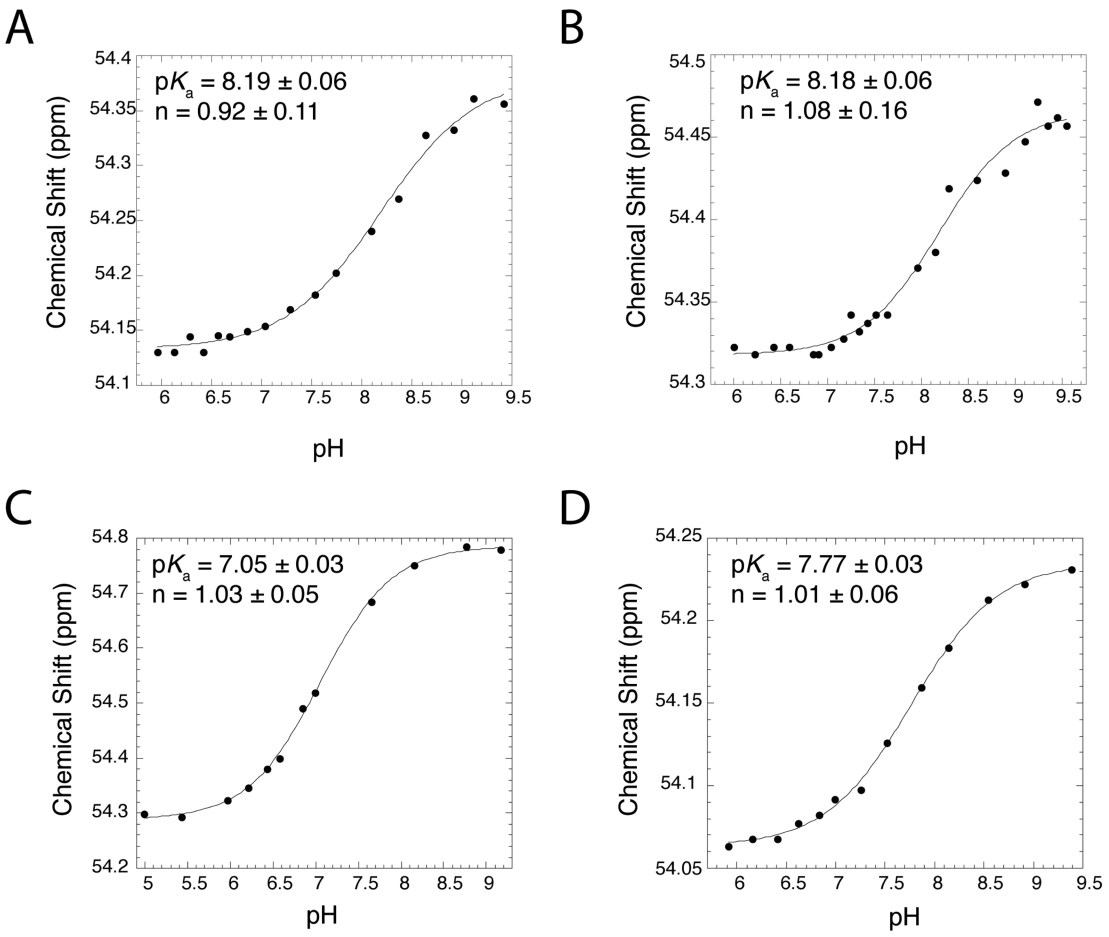

Figure 4. Comparison of standard experimental conditions to biological temperature and Mg^{2+} concentration with ^{31}P NMR-detected pH titrations. The downfield-shifted diastereomer peak is shown, whereas both diastereomer peaks are shown in Figure S6 and S7 of the Supporting Information. (A) pH titration at 37 °C of SS RNA construct. (B) pH titration at 25 °C and biological magnesium concentrations (0.5 mM Mg^{2+}) of SS RNA construct. (C) pH titration at 37 °C of WW′ RNA construct. (D) pH titration at 37 °C of SW′ RNA construct. All titrations are in the background of 100 mM KCl. The pK_a and Hill values are provided in the figure.

dx.doi.org/10.1021/bi400768q | Biochemistry 2013, 52, 7470−7476

25 °C in the SS construct gave a pK_a of 8.14 (Figure S6 of the Supporting Information). This pK_a differs by only 0.04 pK_a units from the Mg^{2+}-free pK_a value at 25 °C, indicating a little to no dependence of pK_a values on physiological Mg^{2+} concentration. The overall absence of a temperature or magnesium dependence for the observed pK_a values suggests that the pK_a values in Table 1 at 25 °C and 100 mM KCl are relevant to physiological temperature and Mg^{2+} conditions.

Potential Roles for pK_a Shifting in Biological Processes. Appreciation of dsRNA's importance in biological processes such as regulation of gene expression by miRNAs,[12−14] RNA editing,[15,16,30] and ribosomal frameshifting[31] is steadily increasing. In RNA editing by ADARs, a preference for editing A's opposite C's has been reported.[30] Wong et al. indicated that the AC preference is due to sterics, selectivity, and the strength of base pairs formed. Positioning an A opposite a purine disfavors editing due to the bulk of the purine, whereas facile editing of an A−U base pair is disfavored because it would lead to nonselective editing. More recently, Kuttan and Bass observed a nearest neighbor dependence of editing the A opposite the C in which an AC with two strong nearest neighbors is edited much more slowly than an AC with one strong and one weak nearest neighbor.[16] They further showed that editing is correlated with the ability of the adenine to be flipped out. We have shown in the present study that a construct in which an A^+·C wobble is flanked by two strong nearest neighbors has a high pK_a, suggesting that an elevated pK_a may lead to less flipping and hence less editing. This suggests the interesting possibility that editing could be tuned by pK_a shifting of an A^+·C wobble as well as by local pH. Additionally, a proton transfer has been proposed between adenine, ADAR residue E396, and a hydrated intermediate, and the pK_a of the A^+·C wobble could affect this process.[15] We hope that the trends presented in the present study will help elucidate the contributions protonated bases make in various dsRNA-mediated processes.

■ CONCLUSIONS

In this study, we have observed a significant dependence of pK_a shifting on nearest neighbors in RNA. Altering the nearest neighbors from two weak A−U base pairs to two strong G−C pairs increased the pK_a by 1.6 units, up to a pK_a value of 8.1. Addition of a bulge two base pairs away from the protonated base pair shifted the pK_a only slightly, but positioning the bulge one base pair away from the protonated base pair perturbed the helical structure and prohibited the protonated base pair from forming. The pK_a values measured herein are shifted well above neutrality, which suggests the possible participation of a protonated adenine in numerous biological processes such as A-to-I editing, miRNA processing, programmed ribosomal frameshifting, and general acid−base catalysis in ribozymes.

■ ASSOCIATED CONTENT

Supporting Information

^{31}P NMR titrations, UV melts, and thermodynamic parameters. This material is available free of charge via the Internet at http://pubs.acs.org.

■ AUTHOR INFORMATION

Corresponding Author

*P. C. Bevilacqua. E-mail: pcb5@psu.edu. Tel: (814) 863-3812.

Present Address

†J. L. Wilcox. Saint Francis University, Department of Chemistry, 216 Science Center, Loretto, PA 15940.

Author Contributions

Experiment design and writing were done by Jennifer L. Wilcox and Philip C. Bevilacqua. Experiments were conducted by Jennifer L. Wilcox. Authors have given approval to the final version of the manuscript.

Funding

Funding was provided by the National Science Foundation (NSF CHE-1213667)

Notes

The authors declare no competing financial interest.

■ ACKNOWLEDGMENTS

The authors thank Professor Scott Showalter and the Penn State NMR facility for assistance with ^{31}P and ^{1}H NMR experiments, including Emmanuel Hatzakis, Wenbin Luo, and John Litner.

■ ABBREVIATIONS

ADAR, adenosine deaminase acting on RNA; dsRNA, double-stranded RNA; SS and SS′, RNAs with two strong G−C nearest neighbor base pairs; SW and SW′, RNAs with one strong G−C and one weak A−U nearest neighbor base pairs; WW and WW′, RNAs with two weak A−U nearest neighbor base pairs; T_m, melting temperature

■ REFERENCES

(1) Saenger, W. (1984) *Principles of nucleic acid structure*, Springer-Verlag, New York.

(2) Legault, P., and Pardi, A. (1997) Unusual dynamics and pK_a shift at the active site of a lead-dependent ribozyme. *J. Am. Chem. Soc. 119*, 6621−6628.

(3) Bevilacqua, P. C., Brown, T. S., Nakano, S., and Yajima, R. (2004) Catalytic roles for proton transfer and protonation in ribozymes. *Biopolymers 73*, 90−109.

(4) Wilcox, J. L., Ahluwalia, A. K., and Bevilacqua, P. C. (2011) Charged nucleobases and their potential for RNA catalysis. *Acc. Chem. Res. 44*, 1270−1279.

(5) Su, L., Chen, L., Egli, M., Berger, J. M., and Rich, A. (1999) Minor groove RNA triplex in the crystal structure of a ribosomal frameshifting viral pseudoknot. *Nat. Struct. Biol. 6*, 285−292.

(6) Nakano, S., Chadalavada, D. M., and Bevilacqua, P. C. (2000) General acid-base catalysis in the mechanism of a hepatitis delta virus ribozyme. *Science 287*, 1493−1497.

(7) Gong, B., Chen, J. H., Chase, E., Chadalavada, D. M., Yajima, R., Golden, B. L., Bevilacqua, P. C., and Carey, P. R. (2007) Direct measurement of a pK_a near neutrality for the catalytic cytosine in the genomic HDV ribozyme using Raman crystallography. *J. Am. Chem. Soc. 129*, 13335−13342.

(8) Nakano, S., and Bevilacqua, P. C. (2007) Mechanistic characterization of the HDV genomic ribozyme: A mutant of the C41 motif provides insight into the positioning and thermodynamic linkage of metal ions and protons. *Biochemistry 46*, 3001−3012.

(9) Nixon, P. L., Cornish, P. V., Suram, S. V., and Giedroc, D. P. (2002) Thermodynamic analysis of conserved loop-stem interactions in P1-P2 frameshifting RNA pseudoknots from plant luteoviridae. *Biochemistry 41*, 10665−10674.

(10) Wilcox, J. L., and Bevilacqua, P. C. (2013) A simple fluorescence method for pK_a determination in RNA and DNA reveals highly shifted pK_a's. *J. Am. Chem. Soc. 135*, 7390−7393.

(11) Siegfried, N. A., O'Hare, B., and Bevilacqua, P. C. (2010) Driving forces for nucleic acid pK_a shifting in an A(+)·C wobble: Effects of helix position, temperature, and ionic strength. *Biochemistry 49*, 3225−3236.

(12) Lau, N. C., Lim, L. P., Weinstein, E. G., and Bartel, D. P. (2001) An abundant class of tiny RNAs with probable regulatory roles in *Caenorhabditis elegans*. *Science 294*, 858−862.

(13) Lagos-Quintana, M., Rauhut, R., Lendeckel, W., and Tuschl, T. (2001) Identification of novel genes coding for small expressed RNAs. *Science 294*, 853−858.
(14) Lee, R. C., and Ambros, V. (2001) An extensive class of small RNAs in *Caenorhabditis elegans*. *Science 294*, 862−864.
(15) Goodman, R. A., Macbeth, M. R., and Beal, P. A. (2012) ADAR proteins: Structure and catalytic mechanism. *Curr. Top. Microbiol. Immunol. 353*, 1−33.
(16) Kuttan, A., and Bass, B. L. (2012) Mechanistic insights into editing-site specificity of ADARs. *Proc. Natl. Acad. Sci. U. S. A. 109*, E3295−3304.
(17) Xia, T., SantaLucia, J., Jr., Burkard, M. E., Kierzek, R., Schroeder, S. J., Jiao, X., Cox, C., and Turner, D. H. (1998) Thermodynamic parameters for an expanded nearest-neighbor model for formation of RNA duplexes with Watson-Crick base pairs. *Biochemistry 37*, 14719−14735.
(18) Mathewc, D. H., Sabina, J., Zuker, M., and Turner, D. H. (1999) Expanded sequence dependence of thermodynamic parameters improves prediction of RNA secondary structure. *J. Mol. Biol. 288*, 911−940.
(19) Moody, E. M., Lecomte, J. T., and Bevilacqua, P. C. (2005) Linkage between proton binding and folding in RNA: A thermodynamic framework and its experimental application for investigating pK_a shifting. *RNA 11*, 157−172.
(20) Moody, E. M., Brown, T. S., and Bevilacqua, P. C. (2004) Simple method for determining nucleobase pK_a values by indirect labeling and demonstration of a pK_a of neutrality in dsDNA. *J. Am. Chem. Soc. 126*, 10200−10201.
(21) Siegfried, N. A., and Bevilacqua, P. C. (2009) Thinking inside the box: Designing, implementing, and interpreting thermodynamic cycles to dissect cooperativity in RNA and DNA folding. *Methods Enzymol 455*, 365−393.
(22) Allawi, H. T., and SantaLucia, J., Jr. (1998) Nearest-neighbor thermodynamics of internal A·C mismatches in DNA: Sequence dependence and ph effects. *Biochemistry 37*, 9435−9444.
(23) Allain, F. H., and Varani, G. (1995) Structure of the P1 helix from group I self-splicing introns. *J. Mol. Biol. 250*, 333−353.
(24) Varani, G., Cheong, C., and Tinoco, I., Jr. (1991) Structure of an unusually stable RNA hairpin. *Biochemistry 30*, 3280−3289.
(25) Proctor, D. J., Kierzek, E., Kierzek, R., and Bevilacqua, P. C. (2003) Restricting the conformational heterogeneity of RNA by specific incorporation of 8-bromoguanosine. *J. Am. Chem. Soc. 125*, 2390−2391.
(26) London, R. E. (1991) Methods for measurement of intracellular magnesium: NMR and fluorescence. *Annu. Rev. Physiol. 53*, 241−258.
(27) Grubbs, R. D. (2002) Intracellular magnesium and magnesium buffering. *Biometals 15*, 251−259.
(28) Alberts, B., Bray, D., Lewis, J., Raff, M., Roberts, K., and Watson, J. D. (1994) *Molecular biology of the cell*, 3rd ed., Garland Science, New York.
(29) Feig, A. L., and Uhlenbeck, O. C. (1999) The role of metal ions in RNA biochemistry, in *The RNA world*, Cold Spring Harbor Press, New York.
(30) Wong, S. K., Sato, S., and Lazinski, D. W. (2001) Substrate recognition by ADAR1 and ADAR2. *RNA 7*, 846−858.
(31) Giedroc, D. P., Theimer, C. A., and Nixon, P. L. (2000) Structure, stability and function of RNA pseudoknots involved in stimulating ribosomal frameshifting. *J. Mol. Biol. 298*, 167−185.